Diabetes, Metabolic Syndrome and Obesity: Targets and Therapy Dovepress
open access to scientific and medical research

Open Access Full Text Article

ORIGINAL RESEARCH

microRNA Expression Profiles in Myocardium of High-Fat Diet-Induced Obesity Rat

This article was published in the following Dove Press journal:
Diabetes, Metabolic Syndrome and Obesity: Targets and Therapy

Huimin Yang*
Xin Xin*
Hang Yu
Yandong Bao
Pengyu Jia
Nan Wu
Dalin Jia

Department of Cardiology, The Central Laboratory, The First Affiliated Hospital of China Medical University, Shenyang, Liaoning, People's Republic of China

*These authors contributed equally to this work

Diabetes, Metabolic Syndrome and Obesity downloaded from https://www.dovepress.com/
For personal use only.

Purpose: A high-fat diet (HFD) can lead to cardiac dysfunction, hypertrophy, and fibrosis. This study aimed to explore microRNA expression profiles in the myocardium of HFD-induced obesity rat.

Materials and Methods: Wistar rats were randomly divided into two groups, and fed with normal chow diet (NCD) or HFD for 20 weeks. Cardiac function was evaluated by echocardiography. Left ventricular myocardium was harvested to assess the extent of myocardial morphology alteration. MicroRNA expression was analyzed using Agilent miRNA microarray and quantitative real-time PCR (qRT-PCR) was used to validate the microarray data. The mirdbV6 database was used to forecast the miRNA target genes. The role of microRNAs in palmitate-induced cardiac hypertrophy and fibrosis in primary neonatal rat cardiomyocytes was evaluated by loss- and gain-of-function experiments.

Results: Significant changes in cardiac function, hypertrophy, fibrosis, and apoptosis were found in HFD rats as compared with NCD rats. miR-141-3p and miR-144-3p were also significantly upregulated in the myocardium of HFD-induced obesity rat. A series of genes involved in essential biological processes, including anatomical structure development and metabolic process, was targeted by these two miRNAs. These target genes were also implicated in signaling pathways involved in the PI3K-Akt signaling pathway, Wnt signaling pathway, autophagy, and protein processing in the endoplasmic reticulum. Inhibition of miR-141 or overexpression of miR-144 attenuated palmitate-induced cardiac hypertrophy and fibrosis. In contrast, overexpression of miR-141 or inhibition of miR-144 aggravated palmitate-induced cardiac hypertrophy and fibrosis.

Conclusion: This study identifies that miR-141 and miR-144 are candidate miRNAs associated with the development of HFD-induced cardiac dysfunction and structure alteration.

Keywords: high-fat diet, obesity, microRNA, cardiac dysfunction, cardiac remodeling

Introduction

In recent years, with the changes in people's diet structure and lifestyle, obesity has gradually become a major threat to human health care globally due to the increased incidence of obesity year by year.[1] It is estimated that global obesity prevalence will reach 18% in men and surpass 21% in women by 2025.[2] It has been found that obesity commonly causes disorders of cardiac metabolism and structure, and is associated with the increased risk for the development of cardiovascular diseases.[3] Recent studies have demonstrated that high-fat diet (HFD)-induced obesity could lead to cardiac dysfunction,[4] hypertrophy,[5] fibrosis,[6] and even heart failure,[7] which is presumably involved in the activation of oxidative stress, inflammation, and apoptosis.[8] However, the elaborate mechanism is not well elucidated.

Correspondence: Dalin Jia; Nan Wu
Department of Cardiology The Central Laboratory, The First Affiliated Hospital of China Medical University, 155th North of Nanjing Street, Heping District, Shenyang, Liaoning 110001, People's Republic of China
Email jdl2001@126.com; imwunan@163.com

© 2020 Yang et al. This work is published and licensed by Dove Medical Press Limited. The full terms of this license are available at https://www.dovepress.com/terms.php and incorporate the Creative Commons Attribution – Non Commercial (unported, v3.0) License (http://creativecommons.org/licenses/by-nc/3.0/). By accessing the work you hereby accept the Terms. Non-commercial uses of the work are permitted without any further permission from Dove Medical Press Limited, provided the work is properly attributed. For permission for commercial use of this work, please see paragraphs 4.2 and 5 of our Terms (https://www.dovepress.com/terms.php).

MicroRNAs, a group of small non-coding RNA, usually function as negative regulators for gene expression via degradation of target messenger RNAs (mRNAs) and/or by repressing their translation.[9] Several recent studies have demonstrated that some aberrant microRNAs, such as microRNA-327,[10] microRNA-155,[11] and microRNA-208a,[12] play key roles in the development of cardiac dysfunction, hypertrophy, and fibrosis. In addition, some specific microRNAs contribute to the regulation of oxidative stress, inflammation, and apoptosis in cardiomyocytes.[13–15] Therefore, we assumed that HFD-induced obesity will lead to aberrant microRNA expression in the myocardium.

To test this hypothesis, our present study detected aberrant microRNA expression in the heart of HFD-induced obesity rats using miRNA microarray and the microarray data was further validated by quantitative real-time PCR (qRT-PCR). The results indicated that miR-141-3p and miR-144-3p were significantly upregulated in obesity rat heart. Moreover, a series of genes involved in essential biological processes, including anatomical structure development and metabolic processes was targeted by these two miRNAs. These target genes were implicated in signaling pathways involved in the PI3K-Akt signaling pathway, the Wnt signaling pathway, autophagy, and protein processing in the endoplasmic reticulum. Lastly, we demonstrated the function of miR-141 and miR-144 on palmitate-induced cardiac hypertrophy and fibrosis in vitro.

Materials and Methods

Animals

A total of thirty male Wistar rats weighing 120±10 g purchased from Liaoning Changsheng Biotechnology Co., Ltd were randomly divided into two groups, and fed normal chow diet (NCD) or HFD (60% kcal) purchased from Beijing HFK Bioscience Co. Ltd for 20 consecutive weeks. All rats were kept at 22–24°C under 12 h light: 12 h dark conditions and had free access to clean water. The bodyweight of rats was monitored twice a week. All experimental procedures adhered to the Guide for the Care and Use of Laboratory Animals (NIH, USA) and were approved by the Institutional Animal Care and Use Committee of China Medical University.

Blood Biochemistry Analysis

To determine the concentration of triglyceride and insulin level, 1 mL blood samples were taken from the rat's tail vein after a 6 h fast, and then the serum values of triglyceride (TG) and insulin were measured using a Triglyceride Assay Kit (Nanjing Jiancheng Bioengineering Institute, catalog No. A110-1-1) and Insulin Assay Kit (Nanjing Jiancheng Bioengineering Institute, catalog No. H203) following the manufacturer's instructions. Glucose tolerance was determined by the intraperitoneal glucose tolerance test. Briefly, the level of fasting blood sugar in overnight-fast rats was detected using Glucose Assay Kit (Nanjing Jiancheng Bioengineering Institute, catalog No. F006-1-1), and then the level of blood sugar was detected again 2 h after administered glucose (1 g/kg, i.p.).

Echocardiography

Rats were anesthetized with inhaled isoflurane (1%) and transthoracic echocardiography was conducted using a Color Ultrasonic Diagnosis System (Vivid E9, GE) and an M-mode Doppler. The parameters of cardiac function including left ventricular end-diastolic diameter (LVEDD), left ventricular end-systolic diameter (LVESD), wall thickness, and fractional shortening were measured.

Histological Analysis

Cardiac tissues were fixed in 4% paraformaldehyde overnight, then embedded in paraffin, and finally divided into 6 μm-thick sections. Tissue sections were performed with hematoxylin and eosin staining to evaluate routine histological analysis of myofibers. To evaluate the deposition of type IV collagen in the myocardium, the sections were also stained with 0.1% Sirius Red F3B and 1.3% saturated aqueous solution of picric acid. Moreover, Masson staining was used to determine the collagen content. As for assessing apoptosis, cardiac tissue sections were performed with the terminal deoxynucleotidyl transferase dUTP nick end labeling (TUNEL) assay using an In Situ Cell Death Detection Kit (Roche, South San Fransisco, CA, USA) following the manufacturer's protocols. TUNEL-positive cells were imaged under a fluorescence microscope.

MicroRNA Microarray Procedures

Sample

Total RNA was extracted from left ventricular myocardium with trizolreagent (TaKaRa) following the manufacturer's recommendations. RNA quantity and quality were measured by NanoDrop ND-1000. RNA integrity was assessed by standard denaturing agarose gel electrophoresis.

Microarray

The Whole Rat miRNA Microarray represents all known miRNAs in the rat transcriptome. Sequences were compiled from a broad source survey, and then verified and optimized by alignment to the assembled rat transcriptome.

RNA Labeling and Array Hybridization

Sample labeling and array hybridization were performed according to the Agilent miRNA Microarray System with miRNA Complete Labeling and Hyb Kit protocol (Agilent Technology). Briefly, total miRNA from each sample was labeled with Cyanine 3-pCp under the action of T4 RNA ligase. The labeled cRNA over the procession of inspissation and desiccation and then redissolved with water. One μg of each labeled cRNA was fragmented by adding 11 μL 10× blocking agent and 2.2 μL of 25× fragmentation buffer, then heated at 60°C for 30 min, and finally 55 μL 2 × GE hybridization buffer was added to dilute the labeled cRNA. Hybridization solution (100 μL) was dispensed into the gasket slide and assembled to the gene expression microarray slide. The slides were incubated for 17 h at 65°C in an Agilent Hybridization Oven. The hybridized arrays were washed, fixed and scanned using the Agilent Microarray Scanner (part number G2505C).

Microarray Analysis

Agilent Feature Extraction software (version 11.0.1.1) was used to analyze the acquired array images. Quantile normalization and subsequent data processing were performed using the GeneSpring GX v14.9 software package (Agilent Technologies). After quantile normalization of the raw data, miRNAs with at least 3 out of 6 samples having flags in Detected ("All Targets Value") were chosen for further data analysis. Differentially expressed miRNAs with statistical significance between the two groups were identified through volcano plot filtering. Differentially expressed miRNAs between the two samples were identified through fold change filtering. Hierarchical clustering was performed using the R scripts.

qRT-PCR

miRNA expression in microarray data was validated by qRT-PCR analysis. Total RNA extracted from the left ventricular myocardium was reverse transcripted to cDNA using a Mir-X™ miRNA First Strand Synthesis Kit (TaKaRa), and then cDNA was conducted by quantitative PCR measurements using Mir-X™ miRNA qRT-PCR SYBR® Kit (TaKaRa) following the manufacturer's protocols. U6 was applied as an internal control for miRNA. To detect mRNA levels of hypertrophy and fibrosis markers (ANP, BNP, collagen I and collagen III) expression, reverse transcription was performed using PrimeScript RT Reagent Kit with gDNA Eraser (TaKaRa, Kusatsu, Japan) and quantitative PCR was performed using SYBR Premix Ex Taq II (TaKaRa) following the manufacturer's protocols. GAPDH was applied as an internal control for mRNA. Primers for qRT-PCR were designed by Sangon Biotech Co., Ltd. (Shanghai, China) (Table 1). The 2-ΔΔCt method was carried out to analyze relative expression.[16]

Target Gene Prediction and Gene Ontology (GO) and Pathway Analysis of Target Genes

The mirdbV6 database (http://mirdb.org/miRDB/) was used to forecast the miRNA target genes. The GO project provides a controlled vocabulary to describe gene and gene product attributes in any organism (http://www.geneontology.org). The ontology includes three domains: biological process, cellular component, and molecular function. Fisher's exact test in Bioconductor's topGO is used to find if there is more overlap between the DE list and the GO annotation list than would be expected by chance. The *p*-value produced by topGO denotes the significance of GO term enrichment in the DE genes. The lower the *p*-value, the more significant the GO Term (*p*-value ≤0.05 is recommended).

Table 1 Information of Primer Sequences

Name	Sequences (5′ to 3′)
rno-miR-144-3p	CCGGGCGTACAGTATAGATGATGTACT
rno-miR-141-3p	CGGCTAACACTGTCTGGTAAAGATGG
rno-miR-3596c	CGCGACTATACAACCTCCTACCTCA
rno-miR-3574	TCAGCCGCTGTCACACG
rno-miR-3541	TCCCTCCCCCTCACTGC
rno-miR-34a-5p	CTGGCAGTGTCTTAGCTGGTTGT
rno-miR-1949	AGGAAGGCGGACATATTAGTCCCT
rno-miR-224	ACGAAATGGTGCCCTAGTGACTACA
rno-miR-18a	GACTGCCCTAAGTGCTCCTTCT
ANP forward	AAAGCAAACTGAGGGCTCTGCTCG
ANP reverse	TTCGGTACCGGAAGCTGTTGCA
BNP forward	AAGTCCTAGCCAGTCTCCA
BNP reverse	GGTCTATCTTCTGCCCAAA
Collagen I forward	ACGTCCTGGTGAAGTTGGTC
Collagen I reverse	CAGGGAAGCCTCTTTCTCCT
Collagen III forward	GTCAGCTGGATAGCGACA
Collagen III reverse	GAAGCACAGGAGCAGGTGTAGA

Pathway analysis is a functional analysis, mapping genes to Kyoto Encyclopedia of Genes and Genomes (KEGG) pathways. The *p*-value (EASE-score, Fisher-*p*-value, or hypergeometric-*p*-value) denotes the significance of the pathway correlated to the conditions. The lower the *p*-value, the more significant is the pathway. (The recommended *p*-value cut-off is 0.05.)

Primary Neonatal Rat Cardiomyocyte Culture

Primary neonatal rat cardiomyocytes were isolated from 1-day-old Wistar rats and cultured as described in our previous study.[17] Briefly, neonatal rats were sacrificed by decapitation and hearts were harvested. The ventricles were further separated and minced into 1 mm^3 pieces, followed by digestion with 0.05% pancreatin and 0.01% collagenase. Then, cardiomyocytes were purified using differential attachment technique and cultured in Dulbecco's modified Eagle medium/F-12 (DMEM/F12) containing 10% FBS, 100 U/mL penicillin, and 100 μg/mL streptomycin. 5-Bromo-2-deoxyuridine (BrdU) (0.1 mM) was added to inhibit non-cardiomyocytes proliferation.

Cell Transfection and Stimulation

MicroRNAs (miRNAs) including miR-141 mimics/miR-144 mimics, miR-141/miR-144 inhibitor, and negative control (NC mimics and NC inhibitor) which were designed and synthesized by GenePharma Co., Ltd (Shanghai, China) were transfected into cells using Lipofectamine 2000 (Invitrogen, Carlsbad, CA, USA) following the manufacturer's instructions and recommendations. At 24 h post-transfection, cells were treated with 200 μM palmitate for 48 h to mimic lipotoxicity in the heart in vitro as described previously.[4]

Immunofluorescence Staining

Primary neonatal rat cardiomyocytes were placed on glass slides. After that, they were fixed with 4% paraformaldehyde for 15 min, permeabilized with 0.1% Triton in PBS for 30 min at room temperature, followed by incubation with blocking solution containing antibody against α-actinin (Abcam, Hong Kong, People's Republic of China) at 4°C overnight for cell surface measurements. After being washed by PBS three times, they were incubated with FITC-conjugated secondary antibody for 30 min at room temperature and detected under the fluorescence microscope.

Statistical Analysis

The results are presented as the mean ± standard error of the mean (SEM). To analyze the differences between the two groups, Student's *t*-test was performed. Differences among more than two groups were initially analyzed using one-way analysis of variance, followed, when appropriate, by multiple comparison analysis using Fisher's least significant difference test. Statistical analysis was performed using SPSS version 17.0 software (SPSS, Inc., Chicago, IL, USA); $p<0.05$ was considered a statistically significant difference.

Results

Significant Changes in Body Weight, Triacylglycerol, Insulin, and Blood Sugar of Rats Fed HFD

After 20 weeks of feeding, the rats fed HFD remarkably outweighed rats fed NCD (Figure 1A). Moreover, the level of triacylglycerol and insulin in rats fed HFD was significantly higher than that in rats fed NCD (Figure 1B and C). The blood glucose level h after glucose intake was also significantly raised in rats fed HFD as compared with rats fed NCD, notwithstanding no significant difference was found in fasting blood glucose between the two (Figure 1D). Taken together, these results suggested that the HFD-induced obesity rat model was established successfully.

HFD-Induced Obesity Deteriorated Cardiac Function

M-mode echocardiography was used to assess the change of cardiac function (Figure 2A). The results of echocardiographic analysis showed that HFD-induced obesity led to an impediment to left ventricular contractile function, as evidenced by a significant increase in LVESD (Figure 2C), with a remarkable deduction in fraction shortening (Figure 2E). However, no significant change in LVEDD was observed (Figure 2B). Moreover, HFD-induced obesity also caused a notable increase in left ventricular wall thickness (Figure 2D), representing a concentric pattern of cardiac hypertrophy. These data suggested that HFD-induced obesity deteriorated cardiac function.

HFD-Induced Obesity Led to Cardiac Hypertrophy, Fibrosis, and Apoptosis

We next examined whether HFD-induced obesity led to myocardial morphology alteration. Cardiomyocyte cross-sectional

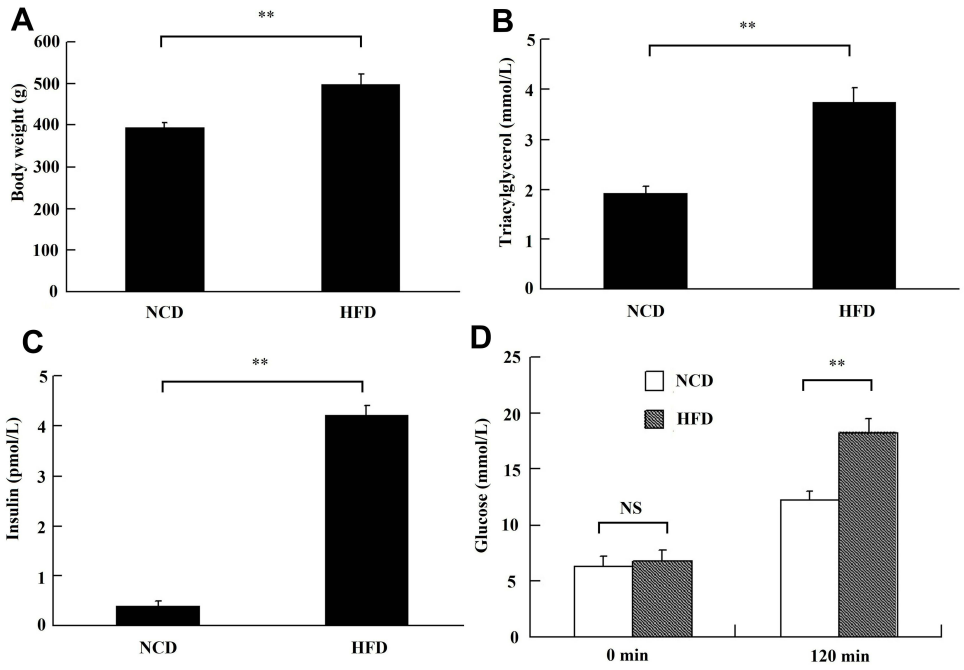

Figure 1 Comparison of body weight, triacylglycerol, insulin, and blood sugar between rats fed high-fat diet (HFD) and rats fed normal chow diet (NCD). (**A**) Bodyweight. (**B**) Serum triacylglycerol level. (**C**) Serum insulin level. (**D**) The intraperitoneal glucose tolerance test (IPGTT). **p<0.01; n=15 per group.
Abbreviation: NS, no significance.

area in HFD group was strikingly larger than that in the NCD group (Figure 3A) and the level of hypertrophy markers (ANP and BNP) was significantly increased in the HFD group as compared with NCD group (Figure 4A and B), which suggested that HFD-induced obesity led to cardiac hypertrophy. Heart sections were stained with Sirius Red and Masson to estimate the extent of fibrosis, and we found that cardiac fibrosis was markedly emerged in the HFD group (Figure 3B and C). The level of fibrosis markers (collagen I and collagen III) was significantly increased in the HFD group as compared with the NCD group (Figure 4C and D). In addition, aberrant apoptosis was found in the HFD group, as evidenced by an increase in TUNEL-positive cells in the myocardium (Figure 3D). Taken together, these results suggested that HFD-induced obesity led to cardiac hypertrophy, fibrosis, and apoptosis.

Aberrant miRNA Expression in Obesity Rat Myocardium

MicroRNA microarray data (GEO database No.: GSE143168) showed that of the 465 detected miRNAs, six microRNAs (rno-miR-141-3p, rno-miR-144-3p, rno-miR-34a-5p, rno-miR-3541, rno-miR-3574, and rno-miR-3596c) were unregulated (log2-ratio >1.5, p<0.05) and three microRNAs (rno-miR-18a-3p, rno-miR-1949 and rno-miR-224-3p) were downregulated (log2-ratio <−1.5, p<0.05) in the HFD group as compared with the NCD group (Figure 5 and Table 2). Above miRNA expressions attained from microarray were further validated by qRT-PCR and the result indicated that the expressions of rno-miR-141-3p and rno-miR-144-3p were significantly increased in the HFD group as compared with the NCD group (Figure 6A and B), but the other miRNAs displayed no significant difference in expression between the HFD group and the NCD group (Figure 6C–I).

Functional Enrichment Analysis of Putative Target Genes

The result of target prediction showed that 482 putative target genes of rno-miR-141-3p and 497 putative target genes of rno-miR-144-3p were predicted. (Supplement-Table 1). We found that 19 target genes of rno-miR-141-3p and 17 target genes of rno-miR-144-3p were mainly involved in the development of cardiac dysfunction, hypertrophy, and fibrosis (Table 3). Moreover, GO analysis of target genes showed that the putative target genes were mainly correlated to functional annotations of anatomical structure development and metabolic process (Figure 7). Simultaneously, pathway enrichment analysis indicated that the predicted target genes were mainly involved in

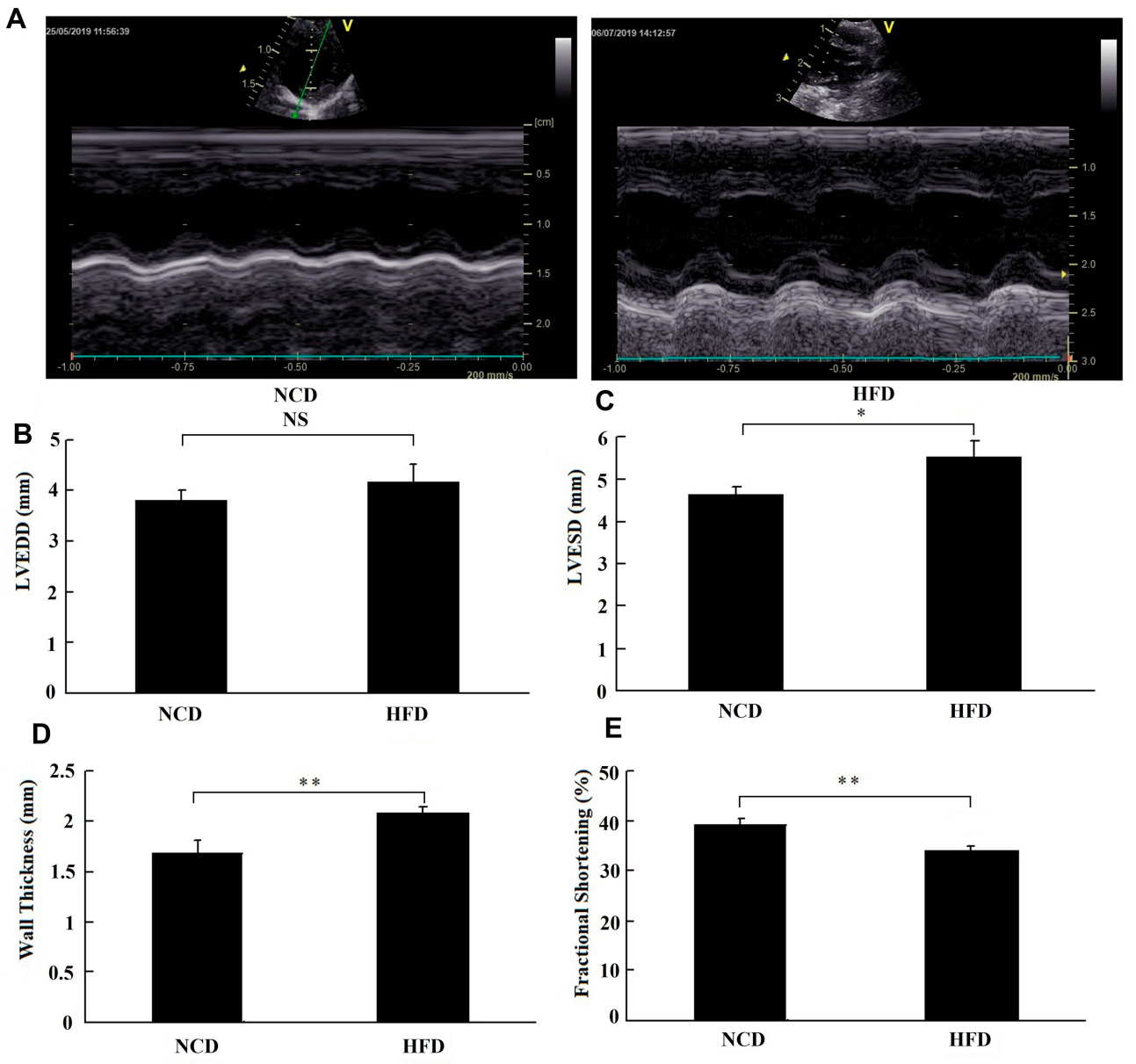

Figure 2 High-fat diet-induced obesity deteriorates cardiac function. (**A**) Representative picture for M-mode. Quantification of left ventricular end-diastolic diameter (LVEDD) (**B**), left ventricular end-systolic diameter (LVESD) (**C**), the wall thickness (**D**), and the fractional shortening (**E**). HFD, rats fed high-fat diet; NCD, rats fed normal chow diet. *p<0.05; **p<0.01; n=15 per group.

Abbreviation: NS, no significance.

the PI3K-Akt signaling pathway, Wnt signaling pathway, autophagy, and protein processing in the endoplasmic reticulum (Figure 8).

Function of miR-141 and miR-144 on palmitate-induced cardiac hypertrophy and fibrosis in vitro

We found that cell surface area was significantly increased after palmitate treatment. Meanwhile, inhibition of miR-141 or overexpression of miR-144 reduced cell surface area in palmitate-treated cardiomyocytes. In contrast, overexpression of miR-141 or inhibition of miR-144 increased cell surface area in palmitate-treated cardiomyocytes (Figure 9A and B). Furthermore, the effect of miR-141 or miR-144 on the change of hypertrophy markers (ANP and BNP) was similar to the result of the cell surface area (Figure 9C and D). In addition, we also detect the effect of miR-141 or miR-144 on the change of fibrosis markers (collagen I and collagen III). The result showed that the level of

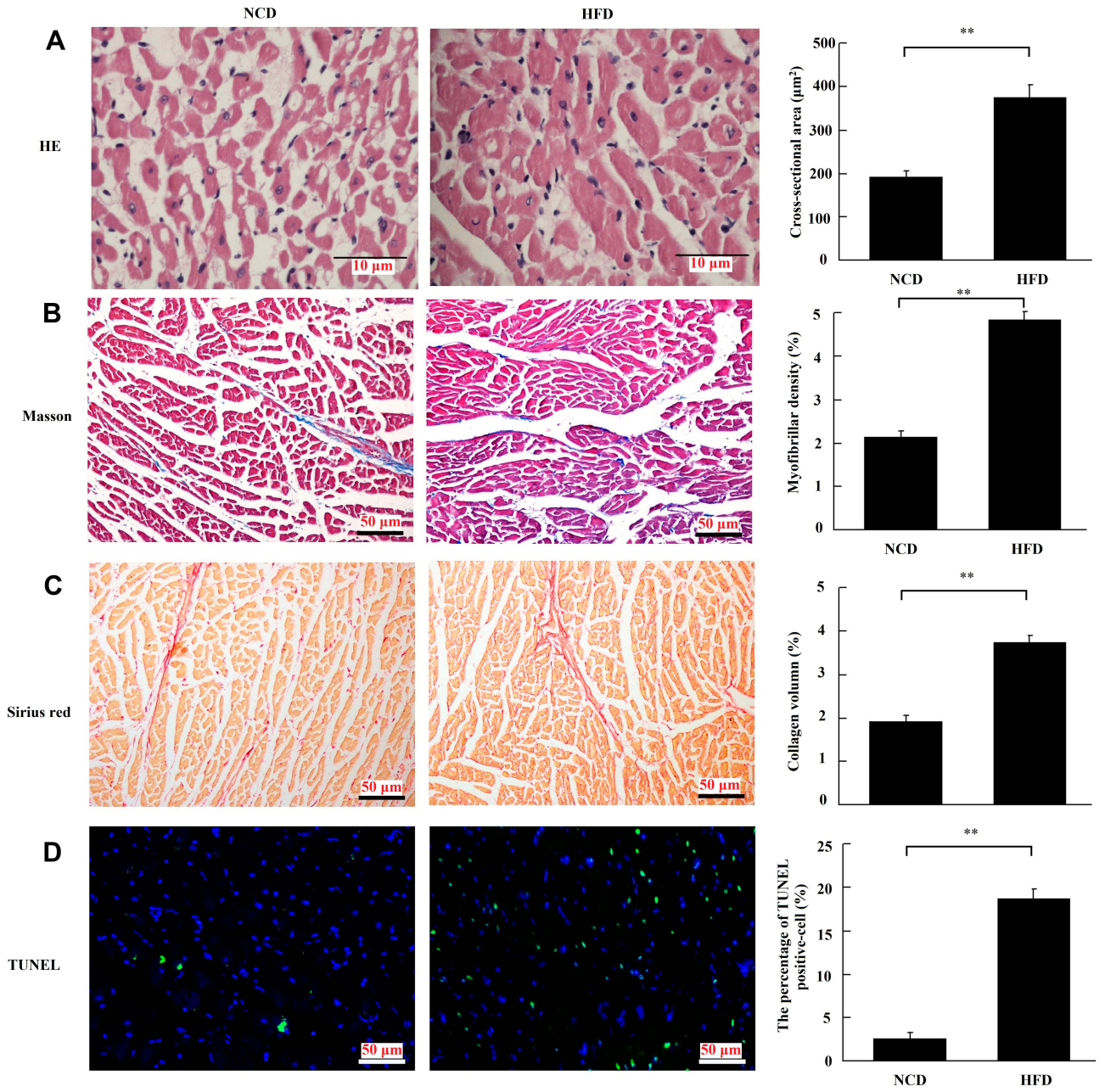

Figure 3 High-fat diet-induced obesity leads to cardiac hypertrophy, fibrosis, and apoptosis. (**A**) Representative picture of hematoxylin and eosin staining (HE) and quantification of the cardiomyocyte cross-sectional area. (**B**) Representative picture of Masson staining and quantification of the myofibrillar density. (**C**) Representative picture of Sirius Red staining and quantification of collagen volume. (**D**) Representative picture of terminal deoxynucleotidyl transferase dUTP nick end labeling (TUNEL) staining and quantification of TUNEL-positive cells. HFD, rats fed high-fat diet; NCD, rats fed normal chow diet. $^{**}p<0.01$, n=6.

collagen I and collagen III in cardiomyocytes was significantly increased after palmitate treatment. Inhibition of miR-141 or overexpression of miR-144 reduced the level of collagen I and collagen III in palmitate-treated cardiomyocytes. Conversely, overexpression of miR-141 or inhibition of miR-144 led to a further increase in the level of collagen I and collagen III in palmitate-treated cardiomyocytes (Figure 9E and F). Taken together, the above results suggested the potential role of miR-141 and miR-144 on palmitate-induced cardiac hypertrophy and fibrosis.

Discussion

Although there is mounting evidence that HFD-induced obesity will lead to cardiac dysfunction, hypertrophy, fibrosis, and even heart failure,[4–7] only few microRNAs have been reported to participate in this process up to now. Kuwabara

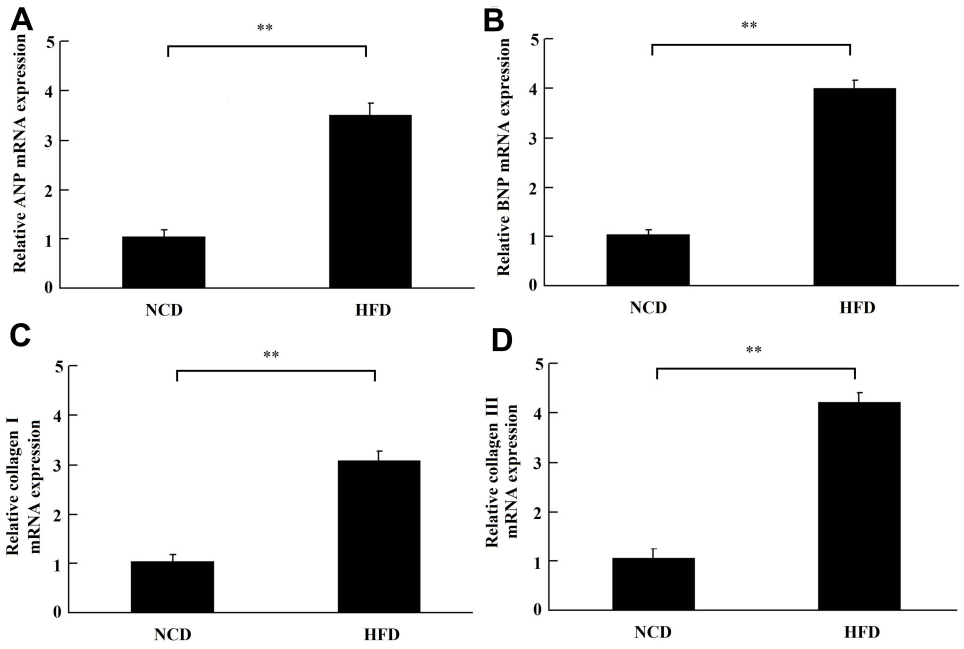

Figure 4 High-fat diet-induced obesity leads to an increase in the mRNA level of mRNA levels of hypertrophy and fibrosis markers. Relative mRNA expressions of ANP (**A**), BNP (**B**), collagen I (**C**) and collagen III (**D**) in myocardium were measured by qRT-PCR. HFD, rats fed high-fat diet; NCD, rats fed normal chow diet. $^{**}p<0.01$, n=6.

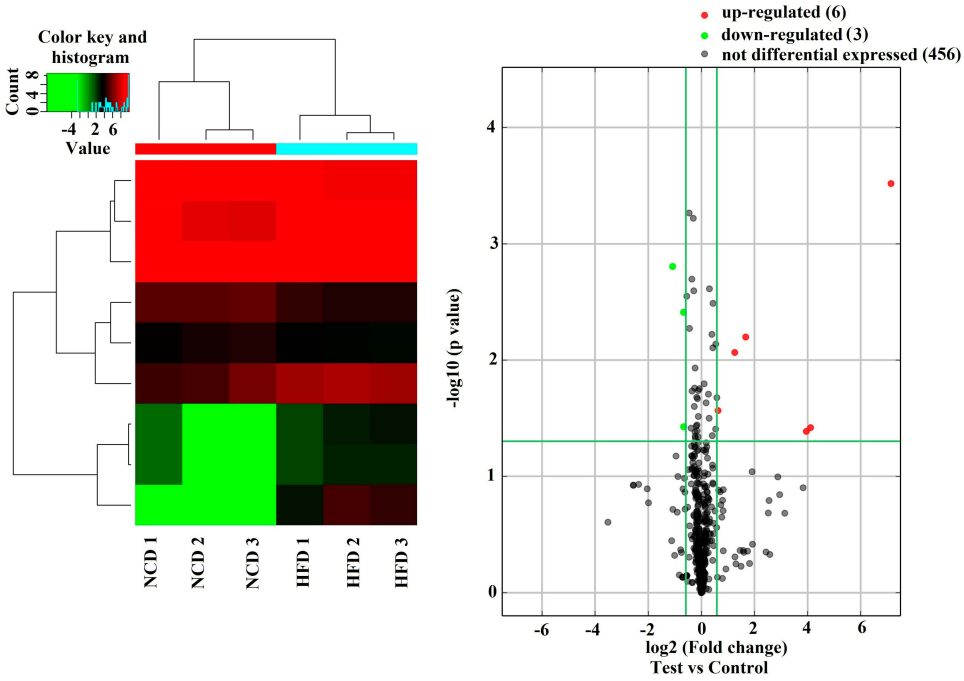

Figure 5 Results of microRNAs microarray analysis of the differentially expressed miRNAs in obesity rat myocardium. (**A**) Heat maps for miRNAs with log2 ratio (HFD/NCD) ≥1.5 or log2 ratio (HFD/NCD) ≤ −1.5 and $p<0.05$. Each row represents a miRNA; differential expression levels were illustrated by the pseudocolor. Red color indicates the transcript levels higher than the median; green = lower; black = equal. (**B**) The analyzed miRNAs are plotted in a volcano plot based on the log2 ratio (HFD/NCD) and *p*-value. A red dot represents a miRNA with log2 ratio (HFD/NCD) ≥1.5 and $p<0.05$; a green dot represents a miRNA with log2 ratio (HFD/NCD) ≤ −1.5 and $p<0.05$. HFD, rats fed high-fat diet; NCD, rats fed normal chow diet.

et al found that knockout of miR-451 in mouse heart could ameliorate HFD-induced cardiac dysfunction and hypertrophy.[5] Zou et al showed that miR-410-5p could exacerbate HFD-induced cardiac fibrosis in mice.[6] As for our research, the results suggested that HFD remarkably induced the expression of miR-141 and miR-144 in rat myocardium, which is consistent with findings in mice, where myocardium remodeling was induced by HFD.[18]

Table 2 Aberrant microRNA Expression in High-Fat Diet-Induced Rat Hearts

microRNA	Fold Change	Regulation	*p*-value
rno-miR-141-3p	3.1806275	Up	0.006
rno-miR-144-3p	2.3882751	Up	0.009
rno-miR-34a-5p	1.5430898	Up	0.027
rno-miR-3541	15.4732195	Up	0.041
rno-miR-3574	17.2719193	Up	0.038
rno-miR-3596c	140.8967477	Up	0.000
rno-miR-18a-3p	1.5849915	Down	0.038
rno-miR-1949	1.591177	Down	0.004
rno-miR-224-3p	2.1171235	Down	0.002

Considering the highly similar results in diverse species, we inferred that the gene function of miR-141 and miR-144 may be highly conserved and crucial to the HFD-induced development of cardiac dysfunction and structure alteration.

It is well accepted that microRNAs exert their roles through degradation of target genes and/or repressing their translation. In other words, if miR-141 and miR-144 contribute to the HFD-induced development of cardiac dysfunction and structure alteration as we inferred, their putative target genes were probably associated with cardiac dysfunction, hypertrophy, and fibrosis. Thus, we speculate the potential function of microRNAs via predicting their target genes. As we expected, in this study, we found that several predicted target genes of miR-141 and miR-144 were associated with cardiac dysfunction, hypertrophy, and fibrosis. This confirmed the potential role of miR-141 and miR-144 in the HFD-induced development of cardiac dysfunction and structure alteration.

Growing evidence has demonstrated that ectopic lipid deposition in heart accounts for the development of cardiac dysfunction and structure alteration of obesity and diabetes induced by HFD.[19,20] HFD-induced obesity or diabetes could lead to mismatches between myocardial fatty acid uptake and utilization,[21] thereby

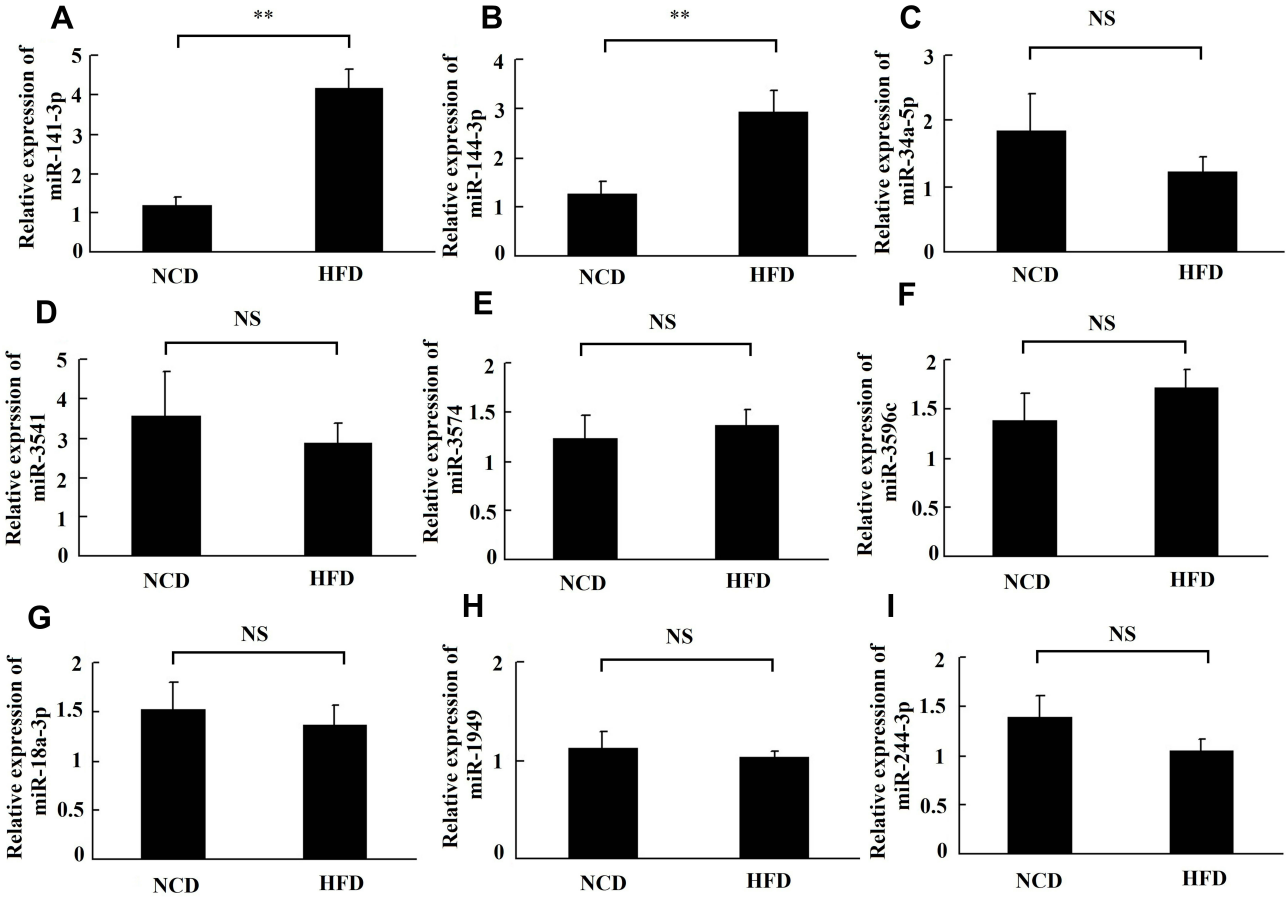

Figure 6 Validation of microarray-based gene expression by qRT-PCR. The relative levels of miR-141-3p (**A**), miR-144-3p (**B**), miR-34a-5p (**C**), miR-3541 (**D**), miR-3574 (**E**), miR-3596c (**F**), miR-18a-3p (**G**), miR-1949 (**H**) and miR-224-3p (**I**). HFD, rats fed high-fat diet; NCD, rats fed normal chow diet. **p<0.01, n=15 per group.
Abbreviation: NS, no significance.

Table 3 Predicted Target Genes for Rno-miR-141-3p and Rno-miR-144-3p

microRNA	Gene Symbol	Gene Name	Gene Function in Heart
rno-miR-141-3p	Thrb	Thyroid hormone receptor beta	Modulation of cardiac hypertrophy
	Ppm1l	Protein phosphatase, Mg2+/Mn2+ dependent, 1L	Modulation of cardiac function
	Brd3	Bromodomain containing 3	Modulation of cardiac hypertrophy
	Peg3	Paternally expressed 3	Modulation of cardiac fibrosis
	Zeb1	Zinc finger E-box binding homeobox 1	Modulation of cardiac fibrosis
	Tiam1	T-cell lymphoma invasion and metastasis 1	Modulation of cardiac hypertrophy
	Rheb	Ras homolog, mTORC1 binding	Modulation of cardiac hypertrophy
	Ube3a	Ubiquitin protein ligase E3A	Modulation of cardiac hypertrophy
	Klf6	Kruppel-like factor 6	Modulation of cardiac fibrosis
	Pkn2	Protein kinase N2	Modulation of cardiac function, hypertrophy and fibrosis
	Grb2	Growth factor receptor bound protein 2	Modulation of cardiac fibrosis
	Cdk6	Cyclin-dependent kinase 6	Modulation of cardiac fibrosis
	Pou4f2	POU class 4 homeobox 2	Modulation of cardiac hypertrophy
	Ezh1	Enhancer of zeste 1 polycomb repressive complex 2 subunit	Modulation of cardiac fibrosis
	Lmbrd1	LMBR1 domain containing 1	Modulation of cardiac hypertrophy
	Ppp2ca	Protein phosphatase 2 catalytic subunit alpha	Modulation of cardiac hypertrophy
	Pacsin2	Protein kinase C and casein kinase substrate in neurons 2	Modulation of cardiac function
	Pln	Phospholamban	Modulation of cardiac hypertrophy
	Gata6	GATA binding protein 6	Modulation of cardiac fibrosis
rno-miR-144-3p	Herpud1	Homocysteine inducible ER protein with ubiquitin like domain 1	Modulation of cardiac hypertrophy
	Smad4	SMAD family member 4	Modulation of cardiac fibrosis
	Hdac2	Histone deacetylase 2	Modulation of cardiac hypertrophy
	Zeb1	Zinc finger E-box binding homeobox 1	Modulation of cardiac fibrosis
	Aplp2	Amyloid beta precursor like protein 2	Modulation of cardiac hypertrophy
	Acsl4	Acyl-CoA synthetase long-chain family member 4	Modulation of cardiac hypertrophy
	Cxcl12	C-X-C motif chemokine ligand 12	Modulation of cardiac fibrosis
	Idh2	Isocitrate dehydrogenase (NADP(+)) 2, mitochondrial	Modulation of cardiac hypertrophy
	Cyp2c11	Cytochrome P450, subfamily 2, polypeptide 11	Modulation of cardiac hypertrophy
	Mmp16	Matrix metallopeptidase 16	Modulation of cardiac fibrosis
	Ezh2	Enhancer of zeste 2 polycomb repressive complex 2 subunit	Modulation of hypertrophy and fibrosis
	Cav3	Caveolin 3	Modulation of cardiac hypertrophy
	Rock2	Rho-associated coiled-coil containing protein kinase 2	Modulation of cardiac function, hypertrophy and fibrosis
	Klf6	Kruppel-like factor 6	Modulation of cardiac fibrosis
	Mtor	Mechanistic target of rapamycin kinase	Modulation of hypertrophy and fibrosis
	Foxo1	Forkhead box O1	Modulation of hypertrophy and fibrosis
	Tlr2	Toll-like receptor 2	Modulation of cardiac fibrosis

promoting the accumulation of cardiotoxic lipid species,[22] and cause lipotoxic cardiomyopathy, manifesting cardiac dysfunction, hypertrophy, and fibrosis.[8] We found that the predicted target genes of miR-144 were enriched in multiple ways of metabolic process. Furthermore, several genes known as the regulators of cardiac fatty acid metabolism, such as Vldlr,[23] Dr1,[24] and Acsl4,[25] were predicted to be target genes of miR-144. This evidence suggested that miR-144 may participate in the development of lipotoxic cardiomyopathy partly via regulating cardiac fatty acid metabolism.

The autophagy pathway plays a key role in the adjustment of the nutritional environment and modulation of numerous metabolic pathways including the reaction to

excessive lipid accumulation.[26] Recent studies have demonstrated that autophagy contributes to the HFD-induced development of cardiac dysfunction and structure alteration.[27,28] For instance, Hsu et al reported that HFD induces cardiomyocyte apoptosis via the inhibition of autophagy in vitro and in vivo.[27] Moreover, Xu and Ren found that HFD-induced cardiac anomalies were associated with Akt-mediated autophagy suppression.[28] In our present study, pathway enrichment analysis indicated that predicted target genes of miR-141 were mainly involved in the PI3K-Akt signaling pathway and autophagy. Although there is a lack of direct evidence based on experimentation, our findings provided a new clue that miR-141 may regulate HFD-induced development of cardiac dysfunction and structure alteration in part via Akt-mediated autophagy.

As excess free fatty acids, such as palmitate, are major mediators of lipotoxicity in the heart and could induce cardiac hypertrophy and fibrosis, we confirmed the role of miR-141 and miR-144 on palmitate-induced cardiac hypertrophy and fibrosis in vitro. To our knowledge, this is the first study to demonstrate the function of miR-141 and miR-144 on palmitate-induced cardiac hypertrophy and fibrosis, which also provided evidence to support the potential role of miR-141 and miR-144 in the HFD-induced development of cardiac dysfunction and structure alteration.

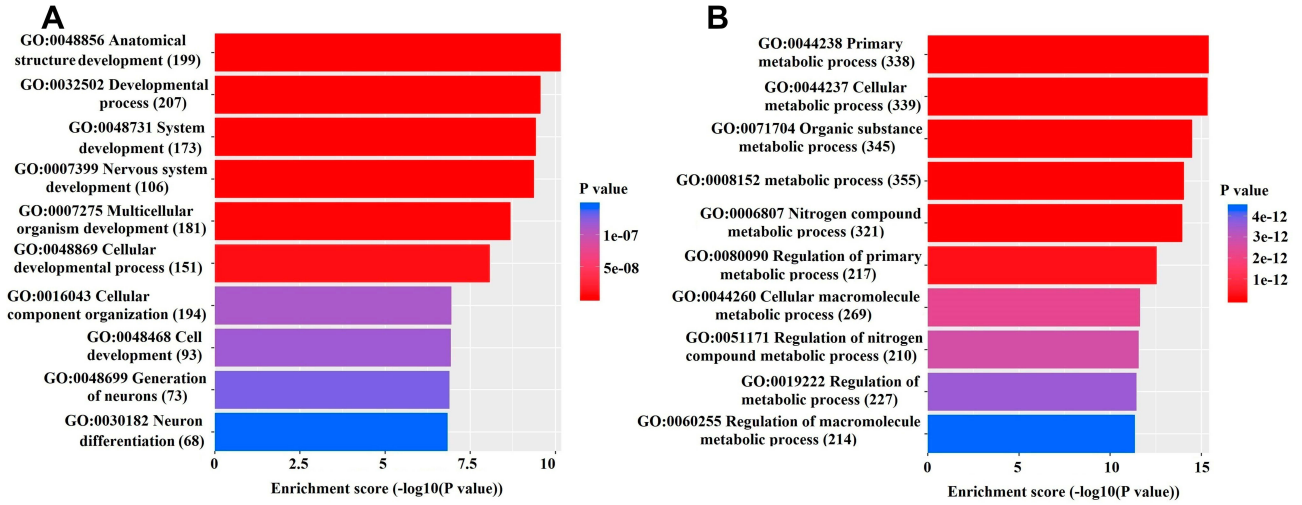

Figure 7 Results of gene ontology (GO) analysis of putative target genes. GO analysis of the putative target genes of miR-141-3p (**A**) and miR-144-3p (**B**). The vertical and horizontal axes represent the biological process and enrichment score for −Log10 (*p*-value) of the corresponding biological process, respectively. The top 10 significant involved GO items ($p<0.001$) are shown.

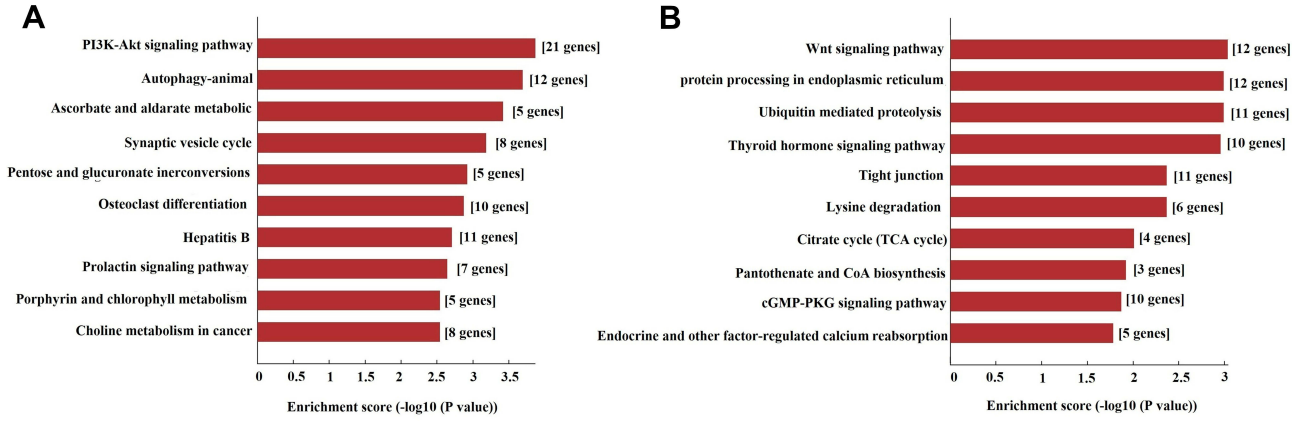

Figure 8 Results of pathway enrichment analysis of putative target genes. Pathway analysis of the putative target genes of miR-141-3p (**A**) and miR-144-3p (**B**). The vertical and horizontal axes represent the pathway and enrichment score for −Log10 (*p*-value) of the corresponding pathway, respectively. The top 10 significant involved pathway items ($p<0.001$) are shown.

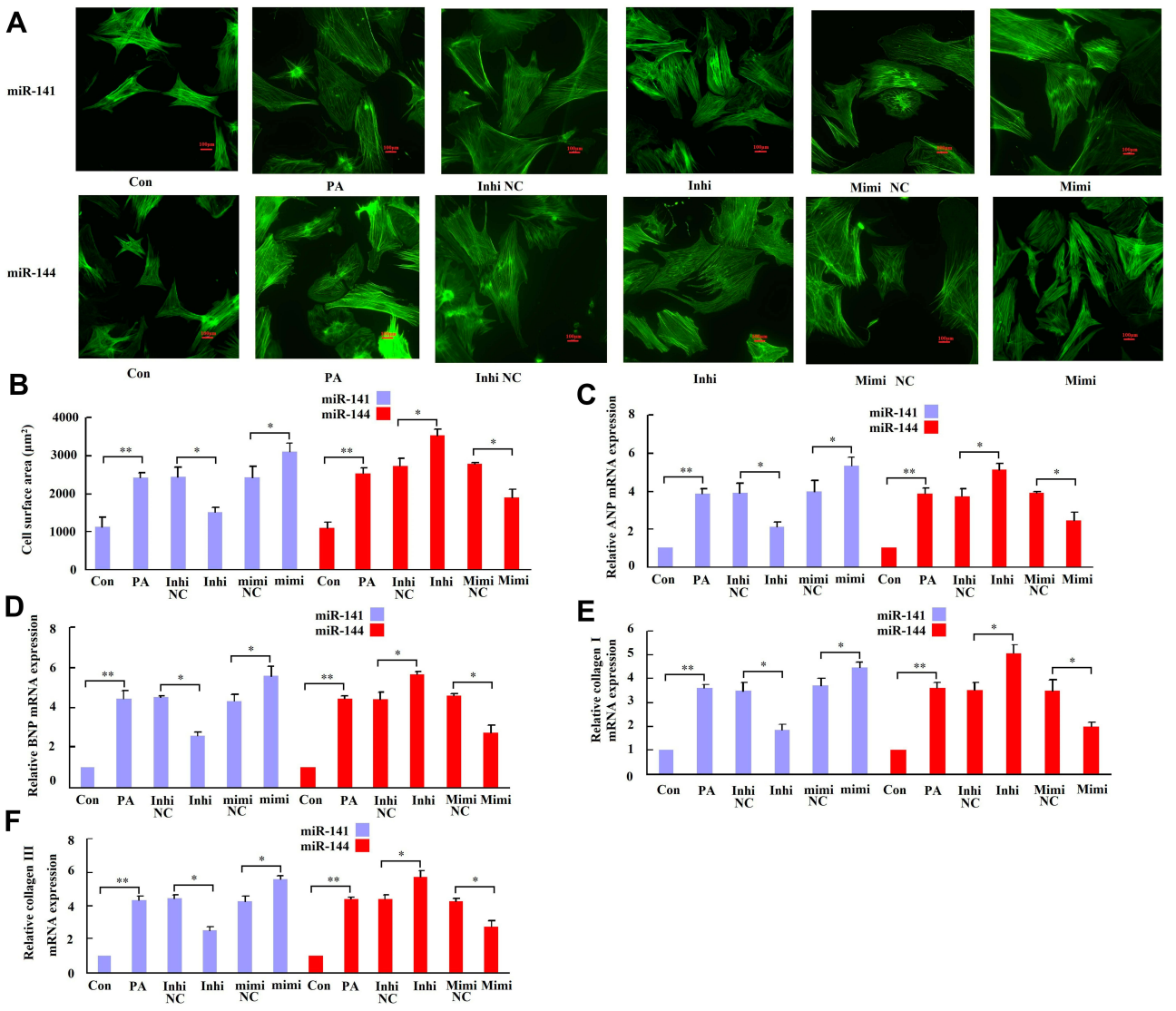

Figure 9 Function of miR-141 and miR-144 on palmitate-induced cardiac hypertrophy and fibrosis in vitro. Primary neonatal rat cardiomyocytes were transfected with miR-141/miR-144 mimics (Mimi), miR-141/miR-144 inhibitor (Inhi), and negative control (NC), followed by treated with 200 μM palmitate (PA) for 48 h. (**A**) α-actinin staining of cross-sectional areas. (**B**) quantification of cross-sectional areas. Relative mRNA expressions of ANP (**C**), BNP (**D**), collagen I (**E**) and collagen III (**F**) in cardiomyocytes were measured by qRT-PCR. Data are presented as the mean ± standard deviation from three independent experiments. *$p<0.05$; **$p<0.01$.

There existed two limitations to our study. Firstly, although we have confirmed the role of miR-141 and miR-144 on palmitate-induced cardiac hypertrophy and fibrosis in vitro, the role of miR-141 and miR-144 in the development of HFD-induced cardiac dysfunction and structure alteration should be further demonstrated in vivo. Another limitation we must acknowledge is that the predicted target genes for miR-141 and miR-144 were not demonstrated by experiments, so they should be further evaluated by qRT-PCR and Western blotting in future study.

Conclusion

This study identifies that miR-141 and miR-144 are candidate miRNAs associated with the HCD-induced development of cardiac dysfunction and structure alteration.

Acknowledgments

This study was supported by the National Natural Science Foundation of China (81800232 and 81670320).

Disclosure

The authors declare that they have no competing interests in this work.

References

1. NCD Risk Factor. Collaboration (NCD-RisC). worldwide trends in body-mass index, underweight, overweight, and obesity from 1975 to 2016: a pooled analysis of 2416 population-based measurement studies in 128·9 million children, adolescents, and adults. *Lancet*. 2017;390(10113):2627–2642.
2. NCD Risk Factor. Collaboration (NCD-RisC). trends in adult body-mass index in 200 countries from 1975 to 2014: a pooled analysis of 1698 population-based measurement studies with 19·2 million participants. *Lancet*. 2016;387(10026):1377–1396. doi:10.1016/S0140-6736(16)30054-X
3. Ortega FB, Lavie CJ, Blair SN. Obesity and cardiovascular disease. *Circ Res*. 2016;118(11):1752–1770. doi:10.1161/CIRCRESAHA.115.306883
4. Xu W, Wang C, Liang M, et al. A20 prevents obesity-induced development of cardiac dysfunction. *J Mol Med (Berl)*. 2018;96(2):159–172. doi:10.1007/s00109-017-1608-3
5. Kuwabara Y, Horie T, Baba O, et al. MicroRNA-451 exacerbates lipotoxicity in cardiac myocytes and high-fat diet-induced cardiac hypertrophy in mice through suppression of the LKB1/AMPK pathway. *Circ Res*. 2015;116(2):279–288. doi:10.1161/CIRCRESAHA.116.304707
6. Zou T, Zhu M, Ma YC, et al. MicroRNA-410-5p exacerbates high-fat diet-induced cardiac remodeling in mice in an endocrine fashion. *Sci Rep*. 2018;8(1):8780. doi:10.1038/s41598-018-26646-4
7. De Pergola G, Nardecchia A, Giagulli VA, et al. Obesity and heart failure. *Endocr Metab Immune Disord Drug Targets*. 2013;13(1):51–57. doi:10.2174/1871530311313010007
8. Sletten AC, Peterson LR, Schaffer JE. Manifestations and mechanisms of myocardial lipotoxicity in obesity. *J Intern Med*. 2018;284(5):478–491. doi:10.1111/joim.12728
9. Iacomino G, Siani A. Role of microRNAs in obesity and obesity-related diseases. *Genes Nutr*. 2017;12:23. doi:10.1186/s12263-017-0577-z
10. Ji Y, Qiu M, Shen Y, et al. MicroRNA-327 regulates cardiac hypertrophy and fibrosis induced by pressure overload. *Int J Mol Med*. 2018;41(4):1909–1916. doi:10.3892/ijmm.2018.3428
11. Seok HY, Chen J, Kataoka M, et al. Loss of MicroRNA-155 protects the heart from pathological cardiac hypertrophy. *Circ Res*. 2014;114(10):1585–1595. doi:10.1161/CIRCRESAHA.114.303784
12. Wang BW, Wu GJ, Cheng WP, Shyu KG. MicroRNA-208a increases myocardial fibrosis via endoglin in volume overloading heart. *PLoS One*. 2014;9(1):e84188. doi:10.1371/journal.pone.0084188
13. Qiu Z, Wang L, Mao H, et al. miR-370 inhibits the oxidative stress and apoptosis of cardiac myocytes induced by hydrogen peroxide by targeting FOXO1. *Exp Ther Med*. 2019;18(4):3025–3031. doi:10.3892/etm.2019.7908
14. Li D, Zhou J, Yang B, Yu Y. microRNA-340-5p inhibits hypoxia/reoxygenation-induced apoptosis and oxidative stress in cardiomyocytes by regulating the Act1/NF-κB pathway. *J Cell Biochem*. 2019;120(9):14618–14627. doi:10.1002/jcb.28723
15. Liu F, Zhang H, Zhang Z, Lu Y, Lu X. MiR-208a aggravates H_2O_2-induced cardiomyocyte injury by targeting APC. *Eur J Pharmacol*. 2019;864:172668. doi:10.1016/j.ejphar.2019.172668
16. Livak KJ, Schmittgen TD. Analysis of relative gene expression data using real-time quantitative PCR and the 2(-Delta Delta C(t)) method. *Methods*. 2001;25:402–408. doi:10.1006/meth.2001.1262
17. Wu N, Zhang X, Bao Y, Yu H, Jia D, Ma C. Down-regulation of GAS5 ameliorates myocardial ischaemia/reperfusion injury via the miR-335/ROCK1/AKT/GSK-3β axis. *J Cell Mol Med*. 2019;23(12):8420–8431. doi:10.1111/jcmm.14724
18. Guedes EC, França GS, Lino CA, et al. MicroRNA expression signature is altered in the cardiac remodeling induced by high fat diets. *J Cell Physiol*. 2016;231(8):1771–1783. doi:10.1002/jcp.25280
19. Van de Weijer T, Schrauwen-Hinderling VB, Schrauwen P. Lipotoxicity in type 2 diabetic cardiomyopathy. *Cardiovasc Res*. 2011;92(1):10–18. doi:10.1093/cvr/cvr212
20. Zlobine I, Gopal K, Ussher JR. Lipotoxicity in obesity and diabetes-related cardiac dysfunction. *Biochim Biophys Acta*. 2016;1861(10):1555–1568. doi:10.1016/j.bbalip.2016.02.011
21. Fukushima A, Lopaschuk GD. Cardiac fatty acid oxidation in heart failure associated with obesity and diabetes. *Biochim Biophys Acta*. 2016;1861(10):1525–1534. doi:10.1016/j.bbalip.2016.03.020
22. Matsui H, Yokoyama T, Sekiguchi K, et al. Stearoyl-CoA desaturase-1 (SCD1) augments saturated fatty acid-induced lipid accumulation and inhibits apoptosis in cardiac myocytes. *PLoS One*. 2012;7(3):e33283. doi:10.1371/journal.pone.0033283
23. Hauton D, Caldwell GM. Cardiac lipoprotein lipase activity in the hypertrophied heart may be regulated by fatty acid flux. *Biochim Biophys Acta*. 2012;1821(4):627–636. doi:10.1016/j.bbalip.2011.12.004
24. Oka S, Zhai P, Yamamoto T, et al. Peroxisome proliferator activated receptor-α association with silent information regulator 1 suppresses cardiac fatty acid metabolism in the failing heart. *Circ Heart Fail*. 2015;8(6):1123–1132. doi:10.1161/CIRCHEARTFAILURE.115.002216
25. Durgan DJ, Smith JK, Hotze MA, et al. Distinct transcriptional regulation of long-chain acyl-CoA synthetase isoforms and cytosolic thioesterase 1 in the rodent heart by fatty acids and insulin. *Am J Physiol Heart Circ Physiol*. 2006;290(6):H2480–H2497. doi:10.1152/ajpheart.01344.2005
26. Jaishy B, Abel ED. Lipids, lysosomes, and autophagy. *J Lipid Res*. 2016;57:1619–1635. doi:10.1194/jlr.R067520
27. Hsu HC, Chen CY, Lee BC, Chen MF. High-fat diet induces cardiomyocyte apoptosis via the inhibition of autophagy. *Eur J Nutr*. 2016;55(7):2245–2254. doi:10.1007/s00394-015-1034-7
28. Xu X, Ren J. Macrophage migration inhibitory factor (MIF) knockout preserves cardiac homeostasis through alleviating Akt-mediated myocardial autophagy suppression in high-fat diet-induced obesity. *Int J Obes (Lond)*. 2015;39(3):387–396. doi:10.1038/ijo.2014.174

Diabetes, Metabolic Syndrome and Obesity: Targets and Therapy Dovepress

Publish your work in this journal

Diabetes, Metabolic Syndrome and Obesity: Targets and Therapy is an international, peer-reviewed open-access journal committed to the rapid publication of the latest laboratory and clinical findings in the fields of diabetes, metabolic syndrome and obesity research. Original research, review, case reports, hypothesis formation, expert opinion and commentaries are all considered for publication. The manuscript management system is completely online and includes a very quick and fair peer-review system, which is all easy to use. Visit http://www.dovepress.com/testimonials.php to read real quotes from published authors.

Submit your manuscript here: https://www.dovepress.com/diabetes-metabolic-syndrome-and-obesity-targets-and-therapy-journal